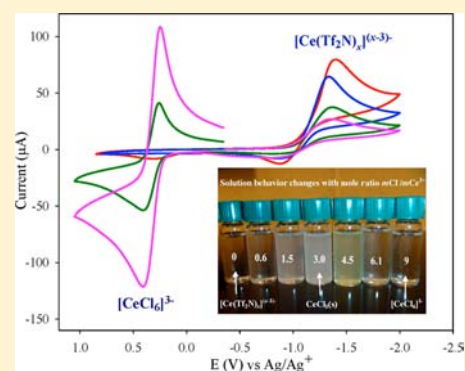


Electrochemical and Spectroscopic Study of Ce(III) Coordination in the 1-Butyl-3-methylpyrrolidinium Bis(trifluoromethylsulfonyl)imide Ionic Liquid Containing Chloride Ion

Li-Hsien Chou, Walter E. Cleland, Jr., and Charles L. Hussey*

Department of Chemistry and Biochemistry, University of Mississippi, Mississippi 38677, United States

ABSTRACT: Cyclic staircase voltammetry, controlled potential coulometry, and electronic absorption spectroscopy were used to probe the coordination and accessible oxidation states of Ce^{3+} dissolved in the ionic liquid 1-butyl-1-methylpyrrolidinium bis(trifluoromethylsulfonyl)imide (BuMePyroTf₂N) before and after the addition of chloride ion as BuMePyroCl. Controlled potential coulometry indicated that the oxidation of Ce metal in this ionic liquid produces only Ce^{3+} . Spectroscopic examination of the resulting solutions indicated that Ce^{3+} was weakly solvated by Tf₂N⁻ ions as $[\text{Ce}(\text{Tf}_2\text{N})_x]^{(x-3)-}$, $x \geq 3$. This species can be reduced at negative potentials, probably to a related Ce^{2+} species, but the latter is unstable and quickly disproportionates to Ce^{3+} and Ce^0 ; the latter appears to react with the ionic liquid. The addition of Cl⁻ to solutions of $[\text{Ce}(\text{Tf}_2\text{N})_x]^{(x-3)-}$ causes the precipitation of $\text{CeCl}_3(\text{s})$, providing a convenient route to the nondestructive recovery of Ce^{3+} from the ionic liquid. However, as the Cl⁻ concentration is further increased, the $\text{CeCl}_3(\text{s})$ redissolves as the octahedral complex, $[\text{CeCl}_6]^{3-}$, and the voltammetric and spectroscopic signature for $[\text{Ce}(\text{Tf}_2\text{N})_x]^{(x-3)-}$ disappears. Absorption spectroscopy indicated that the bulk controlled potential oxidation of solutions containing $[\text{CeCl}_6]^{3-}$ produces $[\text{CeCl}_6]^{2-}$. Although stable on the time scale of voltammetry, this species slowly reacts with the ionic liquid and is converted back to $[\text{CeCl}_6]^{3-}$.



INTRODUCTION

Ionic liquids (ILs) are defined by consensus as molten salts that are liquid below 100 °C. Compared to conventional organic solvents, ILs exhibit several advantages, including minimal vapor pressure, significant thermal stability, and nonflammability. The physical, chemical, and electrochemical properties of these ionic solvents depend strongly on the particular organic cations and anions from which they are prepared. These aspects of ionic liquids as they relate to their use as solvents for electrochemistry have been discussed at length in recent monographs^{1,2} and reviews.^{3,4} Although a seemingly infinite array of cations and anions from which to prepare ILs now exists, a very versatile, easily synthesized hydrophobic IL with a wide electrochemical window and substantial liquidus range is obtained by the association of 1-butyl-1-methylpyrrolidinium cations (BuMePyro⁺) with bis(trifluoromethylsulfonyl)imide anions (Tf₂N⁻).⁵ The resulting BuMePyroTf₂N salt has a melting point of -18 °C. The physical and transport properties of this IL and those of five similar Tf₂N⁻-based ILs were recently reported.^{6,7} From the standpoint of electronic absorption spectroscopy, this ionic solvent has a definite advantage over the aromatic imidazolium-based IL systems⁸ by virtue of its extended UV-cutoff, which is comparable to that of aliphatic alcohols.

The processing of spent nuclear fuel (SNF) results in large quantities of toxic, radioactive waste containing in addition to Pu and U minor actinides, such as Am, Cm, and Np, as well as trivalent lanthanides. There is considerable interest in replacing

the inflammable volatile organic solvents normally used for the liquid–liquid separation of actinide and lanthanide fission products with ILs, which offer many obvious safety advantages.^{9,10} Although many investigations of lanthanides and actinides have been carried out in ILs,^{11–13} there is still uncertainty about the coordination, accessible oxidation states, redox potentials, and transport properties of lanthanide and actinide solutes in these solvents.

Cerium is somewhat unique among the lanthanides because it is one of few such elements with a stable 4+ oxidation state. Because of the close correspondence of the ionic radius of Ce to that of Pu in an eight-coordination environment (Ce⁴⁺ 97 pm and Pu⁴⁺ 96 pm),¹⁴ some similarities between their chemistries, and the significant radiological toxicity of the latter, Ce is often used as a surrogate for Pu. For example, Ce was recently used as a substitute for Pu to assess the hydrothermal stability of the zirconolite phase in SynRoc, which is a synthetic ceramic material intended for the sequestration of radioactive waste.¹⁵ In addition, Ce⁴⁺ has been found to be a valuable reagent for the oxidative transformation of organic compounds in ionic liquids. However, effective methods for converting the Ce³⁺ resulting from these reactions to Ce⁴⁺ have remained elusive.¹⁶ Cerium is also produced during the fission of ²³⁹Pu and ²³⁵U, with the medium-lived ¹⁴¹Ce and ¹⁴⁴Ce, being particularly problematic to human health.

Received: June 1, 2012

Published: October 24, 2012



There is a surprising paucity of information about the electrochemistry and/or coordination of cerium in ionic liquids. A previous investigation that was conducted in the Lewis basic or chloride-rich $\text{AlCl}_3\text{-EtMeImCl}$ ionic liquid indicated that the chemistry of Ce^{4+} and Ce^{3+} is dominated by the $[\text{CeCl}_6]^{2-}$ and $[\text{CeCl}_6]^{3-}$ anions, respectively.¹⁷ Although kinetically stable in water containing chloride in the absence of a catalyst,¹⁸ the former reacts slowly with unbound Cl^- in this ionic liquid. The electronic spectra of these species in chloride-rich $\text{AlCl}_3\text{-EtMeImCl}$ were quite similar to those reported by Ryan and Jorgensen in Et_4NCl -saturated CH_3CN .¹⁹ More recently, the electrochemistry of $\text{Ce}^{4+/3+}$ was examined in BuMeImCl over the temperature range extending from 343 to 373 K.²⁰ As anticipated, given the coordination environment afforded by this ionic liquid, the electrochemistry of cerium is dominated by the $[\text{CeCl}_6]^{2-/3-}$ electrode reaction. By contrast, Ce^{3+} can be reduced directly to the metal in a single three-electron step in classical halide-based molten salts (or high melting ionic liquids), such as LiF-CaF_2 at 1093 K.²¹

In this article, we report an investigation of the electrochemistry and electronic absorption spectroscopy of Ce^{3+} in the $\text{BuMePyroTf}_2\text{N}$ ionic liquid before and after the addition of Cl^- . Many metal ions, including actinides and lanthanides, are soluble in Tf_2N^- -based ILs as a result of the weakly coordinating environment provided by interactions with the oxygen atoms of this anion.²² In fact, molecular dynamics simulations suggest that the coordination number of Eu^{3+} in $\text{BuMeImTf}_2\text{N}$ is around 9–10.²³ Homoleptic compounds of the type $\text{BuMePyro}_2[\text{Ln}(\text{Tf}_2\text{N})_5]$, $\text{Ln} = \text{Nd}^{3+}$, Pr^{3+} , and Tb^{3+} , with the lanthanide cations coordinated to nine oxygen atoms by one monodentate and four bidentate Tf_2N^- ligands have been isolated from the $\text{BuMePyroTf}_2\text{N}$ ionic liquid.^{24,25} However, Cl^- is a much stronger ligand than Tf_2N^- and would be expected to displace the latter from the lanthanide coordination sphere. Thus, the addition of Cl^- to solutions of Ce^{3+} in $\text{BuMePyroTf}_2\text{N}$ is expected to result in a dramatic change in the Ce^{3+} solvation environment, which should be reflected by changes in the voltammetry and electronic absorption spectroscopy of these solutions.

EXPERIMENTAL SECTION

The preparation and purification of BuMePyroCl was carried with a modification of the classical method used to prepare 1,3-dialkylimidazolium chloride salts.²⁶ The 1-methyl pyrrolidine (Aldrich, 97%) starting material was vacuum distilled from $\text{Ca}(\text{OH})_2$ and refluxed with a large excess of 1-chlorobutane (Aldrich $\geq 99.8\%$) in acetonitrile at 80 °C for 72 h. Upon cooling, yellowish-white crystals of BuMePyroCl were obtained. The crude product was dissolved in acetonitrile and crystallized by adding ethyl acetate; excess solvent was removed by filtration. Finally, the crystals were washed with small amounts of ethyl acetate and dried under vacuum overnight.

$\text{BuMePyroTf}_2\text{N}$ was prepared by adding BuMePyroCl to an equal molar amount of lithium bis(trifluoromethylsulfonyl)imide dissolved in water with stirring for a minimum of 24 h. The resulting $\text{BuMePyroTf}_2\text{N}$ was extracted with dichloromethane and washed repeatedly with water in a separatory funnel until no chloride could be detected by the silver nitrate test (voltammetry was also used to test for the presence of chloride, see for example the voltammograms of Cl^- in Figure 8). The dichloromethane solution of $\text{BuMePyroTf}_2\text{N}$ was passed through a column of activated alumina and evacuated in a rotary evaporator to remove the solvent. The last traces of dichloromethane and water were removed by heating the ionic liquid to 60 °C at a pressure of 1×10^{-4} Torr for 36 h. The final product was a colorless liquid with a water content of less than 1 ppm as determined with a Brinkman 756 Karl Fischer coulometer.

Cerium metal (Alfa AESAR, 99.98%) was used as purchased. Because of the significant reactivity of Ce metal with moisture and oxygen, all experiments were carried out in a Vacuum Atmospheres Co. Nexus nitrogen-filled glovebox with H_2O and $\text{O}_2 < 5$ ppm. Electrochemical experiments were carried out with an EG&G PARC Model 263A potentiostat/galvanostat controlled by EG&G PARC Model 270 software (version 2) running on a PC. Electronic positive feedback resistance compensation was employed during all electrochemical experiments. A Pine Instrument Co. Teflon-shrouded platinum disk electrode (geometrical surface area = 0.196 cm^2) served as the working electrode. The electrode was polished successively with 1.0, 0.3, and 0.05 μm alumina (Buehler) on a Buehler Metaserv grinder-polisher, washed with distilled water, and dried in the glovebox antechamber before use. A Bioanalytical Systems MF-2042 non-aqueous Ag^+/Ag electrode served as the reference electrode. The potential of the Fc^+/Fc couple was 0.061 V versus this reference. The counter electrode consisted of a platinum wire spiral immersed in $\text{BuMePyroTf}_2\text{N}$, but separated from the bulk IL by a porosity E glass frit (ACE Glass). The temperature of the electrochemical cell was controlled to 323 ± 1 K with a small hot plate/stirrer.

Absorption spectra were acquired outside the glovebox in 2-mm path length fused silica cells fitted with airtight Teflon caps by using a Shimadzu UV-1600 UV-visible spectrophotometer. X-ray diffraction (XRD) measurements were carried out with a Shimadzu XD-D1 diffractometer. X-ray photoelectron spectroscopy (XPS) was performed with a VG Science, Ltd., ESCA 210 equipped with an Al ($K\alpha$) standard X-ray source operating at 1486.6 eV. Binding energy (BE) data were calibrated to C 1s at 284.6 eV. Both XRD and XPS measurements were carried out at the NSC Instrument Center at National Cheng Kung University in Taiwan. Elemental chemical analysis (C, Cl, F, H, N) was performed by Galbraith Laboratories, Inc., Knoxville, TN.

RESULTS AND DISCUSSION

Coulometric Oxidation of Ce. To avoid the introduction of foreign anions during the dissolution of cerium in $\text{BuMePyroTf}_2\text{N}$, Ce^{n+} was introduced into the ionic liquid by the oxidation of Ce metal at a potential of 0.8 V in a divided cell. The oxidation state, n , of the dissolved Ce^{n+} species was calculated from the change in the weight, Δw , of the Ce metal electrode after the passage of a given charge, Q_{exp} , by using Faraday's law,

$$n = 140.12 Q_{\text{exp}} / F \Delta w \quad (1)$$

where F is the Faraday constant. The results of these experiments are given in Table 1, and they clearly indicate

Table 1. Anodic Dissolution of a Ce Electrode in the $\text{BuMePyroTf}_2\text{N}$ Ionic Liquid at an Applied Potential of 0.75 V

Δw (g)	Q_{exp} (C)	n
0.0211	45.0	3.09
0.0197	41.0	3.02
0.0161	34.7	3.05

that the species introduced by using this procedure is Ce^{3+} . Because this coulometric method for introducing Ce^{3+} into the ionic liquid is not based on the dissolution of a compound or complex with attendant anions and because no appreciable concentration of water is present in the ionic liquid, the resulting soluble Ce^{3+} species must be solvated or coordinated by Tf_2N^- anions. Therefore, we investigated the coordination of Ce^{3+} by using electronic absorption spectroscopy.

Electronic Absorption Spectroscopy of Ce^{3+} in $\text{BuMePyroTf}_2\text{N}$. Absorption spectra for solutions of Ce^{3+} in

BuMePyroTf₂N that were recorded at different concentrations are shown in Figure 1. These spectra exhibit four moderately

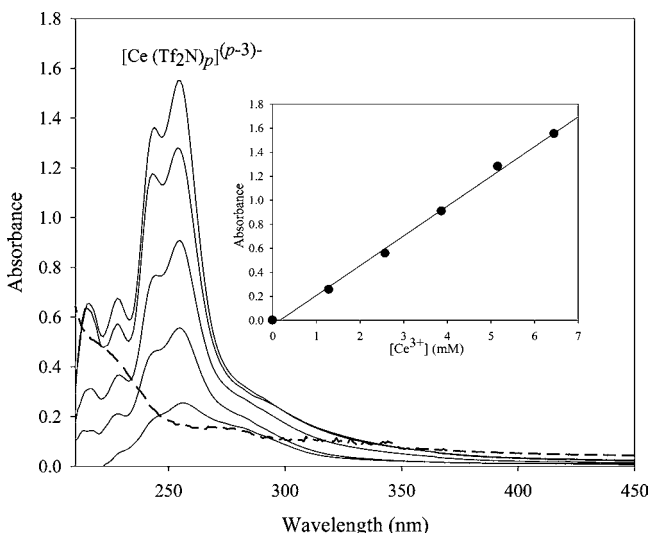


Figure 1. Electronic absorption spectra in BuMePyroTf₂N: (---) neat ionic liquid versus air; (—) Ce³⁺ as a function of concentration. Inset: Plot of the absorbance at 254 nm versus the Ce³⁺ concentration.

intense absorption bands at 254 nm (1160 l mol⁻¹ cm⁻¹), 244 nm (990 l mol⁻¹ cm⁻¹), 228 nm (470 l mol⁻¹ cm⁻¹), and 216 nm, as well as a poorly resolved shoulder at about ~290 nm. (No molar absorptivity value is given for the 216 nm band, because the absorbance of this band cannot be measured accurately due to its proximity to the UV-cutoff of the ionic liquid.) The inset of this figure illustrates that the band at 254 nm obeys the Lambert–Beer law. These spectra are very similar in appearance, especially with regard to the band profiles and relative intensities, to that reported for weakly solvated Ce³⁺ in aqueous 1.0 M HClO₄, where bands are observed at 253 nm (705 l mol⁻¹ cm⁻¹), 240 nm (600 l mol⁻¹ cm⁻¹), 222 nm (360 l mol⁻¹ cm⁻¹), and 211 nm (270 l mol⁻¹ cm⁻¹);²⁷ these bands have been attributed to 4*f* → 5*d* electronic transitions. Note that in aqueous solutions, a fifth band is reported at 200 nm for Ce³⁺,²⁷ but if present in the ionic liquid solutions, this band would appear below the UV-cutoff of the solvent. In addition, a weak band is reported at 297 nm in aqueous solution, but this band is not attributed to a *f* → *d* transition. The shoulder that we observe at 290 nm may correspond to this band. Thus, despite the differences in the solvating ligands, the concordance between the spectroscopic results found in the ionic liquid and those reported in aqueous HClO₄ provides strong evidence that Ce³⁺ is only weakly solvated in BuMePyroTf₂N, probably in the form of species such as [Ce(Tf₂N)_{*x*}]^{(*x*-3)⁻, most likely with *x* = 5. This conclusion is supported by the aforementioned isolation of homoleptic compounds of the type [BuMePyro]₂[Ln(Tf₂N)₅] (Ln = Nd, Pr, and Tb).^{24,25} Recent EXAFS and MD calculations also support this conclusion.²⁸}

Cyclic Voltammetry of Ce³⁺ in BuMePyroTf₂N. Cyclic staircase voltammograms (CSV) recorded at a Pt electrode in BuMePyroTf₂N with and without added Ce³⁺ are shown in Figure 2. The former voltammogram exhibits three well-defined waves; one large reduction wave with a cathodic peak potential, *E*_p^c, of about -1.34 V, and two associated oxidation waves located at *E*_p^a ≈ -0.8 and ~0.4 V, respectively. Figure 3 (top)

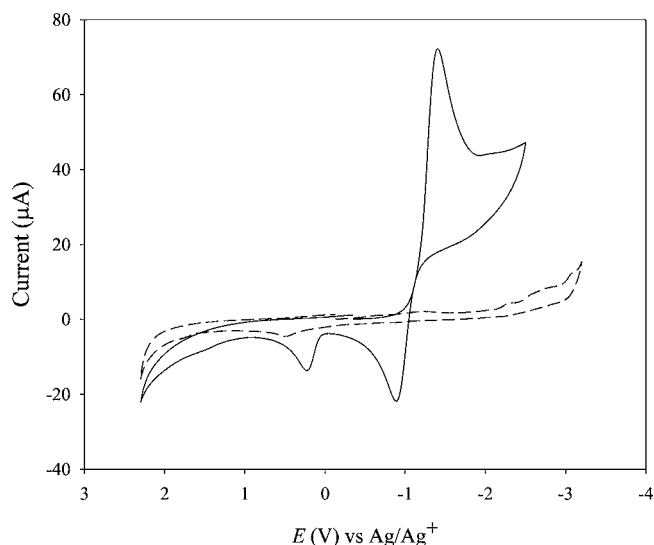


Figure 2. Cyclic staircase voltammograms recorded at a Pt electrode in BuMePyroTf₂N: (---) pure ionic liquid; (—) 0.095 M Ce³⁺. The scan rates were 50 mV s⁻¹.

indicates that at a fixed scan rate the peak current for the reduction wave at -1.34 V scales linearly with the Ce³⁺ concentration, confirming that this wave arises from the reduction of Ce³⁺.

Comparison of the voltammograms in Figures 2 and 3 with those reported for the reduction of several other trivalent lanthanides with stable divalent oxidation states, such as Eu³⁺, Sm³⁺, and Yb³⁺ dissolved in this and related Tf₂N⁻-based ionic liquids,^{29–31} suggests that the reduction wave and first oxidation wave in these voltammograms corresponds to the Ce^{3+/2+} electrode reaction. However, it is obvious from inspection of the voltammograms in these figures that the current for the oxidation wave at *E*_p^a ≈ -0.8 V is much smaller than expected for a chemically stable system, that is, the ratio of the oxidation peak current to the reduction peak current, *i*_p^a/*i*_p^c, is considerably less than one. This suggests that the Ce³⁺ reduction reaction is not a simple process, but involves homogeneous chemistry coupled to the charge transfer process.

Figure 3 (bottom) shows a series of voltammograms that were recorded at different scan rates at a fixed concentration of Ce³⁺. The data taken from these voltammograms are collected in Table 2. As shown in the inset of this figure, the peak current function, *i*_p^c/ν^{1/2}, decreases by about 30% as the scan rate is increased from 0.010 to 0.300 V s⁻¹. Furthermore, as the scan rate is increased, *E*_p^c for the wave at -1.34 V shifts toward more negative potentials. Taken together, these results are consistent with a coupled chemical step involving disproportionation of the primary product of the charge transfer reaction.³² A reasonable explanation for these results is provided by the following reaction sequence in which the charge transfer product, Ce²⁺, undergoes rapid disproportionation to Ce³⁺ and Ce⁰



This result is not unexpected because cerium does not exhibit any significant divalent chemistry, and no verified divalent compounds appear to have been isolated. Furthermore, it is doubtful that the Ce⁰ produced during this

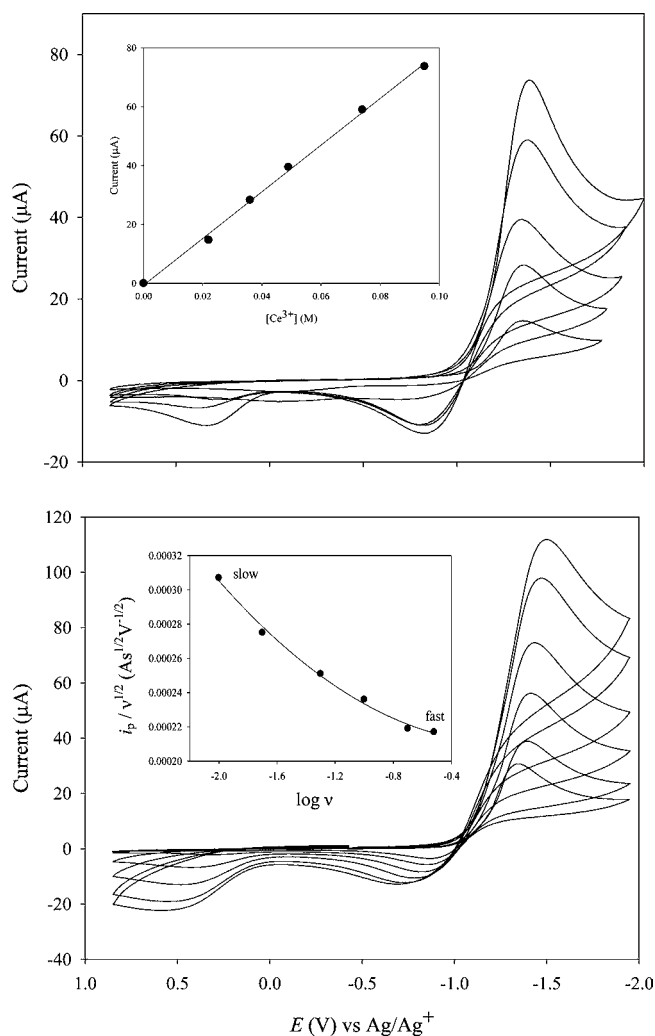


Figure 3. Cyclic staircase voltammograms recorded at a Pt electrode in BuMePyroTf₂N. Top: 0.020, 0.035, 0.050, 0.075, and 0.095 M Ce³⁺; the scan rates were 50 mV s⁻¹. Inset: Plot of the reduction peak current versus the Ce³⁺ concentration. Bottom: voltammograms recorded at a Pt electrode in BuMePyroTf₂N containing 0.095 M Ce³⁺ as a function of scan rate. Inset: relationship between the peak current function and the logarithm of the scan rate.

Table 2. Cyclic Staircase Voltammetric Data for the Ce^{3+/2+} Reaction in BuMePyroTf₂N

ν (V s ⁻¹)	E_p^c (V)	$10^5 i_p$ (A)	$10^4 i_p / \nu^{1/2}$ (A s ^{1/2} V ^{-1/2})	i_p^a / i_p^c
0.01	-1.344	3.07	3.07	0.481
0.02	-1.394	3.89	2.75	0.530
0.05	-1.414	5.62	2.51	0.552
0.10	-1.434	7.45	2.36	0.553
0.20	-1.474	9.79	2.19	0.569
0.30	-1.498	11.19	2.17	0.567

reaction is thermodynamically stable because we were unable to obtain any evidence for the deposition or formation of metallic Ce⁰ on the electrode (vide infra). This result is counterintuitive to the observation that bulk Ce⁰ electrodes, such as the Ce⁰ coupons we routinely use to prepare solutions of Ce³⁺ by anodic oxidation (vide supra), seem to be stable at room temperature in the ionic liquid for extended periods of time. A reasonable explanation for this result is that Ce⁰ reacts with the component ions of the ionic liquid to form a solid electrolyte

interface (SEI) layer similar to that found when Li⁰ is immersed in ionic liquids.³³ This passivating SEI layer prevents further reaction with the solvent (and in the case of Li⁰ makes lithium-ion batteries possible). However, Ce⁰ produced during the disproportionation of Ce²⁺ is another matter because it is expected to be finely divided and therefore highly reactive.

To test this possibility further, we conducted a series of bulk electrolysis experiments with ionic liquid solutions of Ce³⁺ at a large surface area Pt electrode at an applied potential of -1.75 V. During the course of these experiments, the electrode surface became fouled with an unidentifiable insoluble, passivating material. The activity of the electrode could only be restored if its surface was thoroughly cleaned with a suitable organic solvent, such as CH₂Cl₂ or CH₃CN. This electrode surface film undoubtedly resulted from the disproportionation reaction because no electrochemical reactions are expected at this potential, cf. the background voltammogram in Figure 2. In fact, the second oxidation wave at $E_p^a \sim 0.4$ V in Figures 2 and 3 may be due to oxidation of the product resulting from the reaction of Ce⁰ with the ionic liquid.

Amperometric Titration: Addition of Cl⁻ to Solutions of Ce³⁺. The coordination of Ce³⁺ by chloride in BuMePyroTf₂N was probed by conducting amperometric titration experiments in which CSV was used to monitor the reduction and oxidation currents of the species of interest. In the first of these experiments, the peak voltammetric currents for the reduction of Ce³⁺ in a solution containing a fixed amount of this species were recorded at the same scan rate after the addition of weighed portions of BuMePyroCl. Some examples of the voltammograms that resulted from these experiments are given in Figure 4. The graphical results are depicted in Figure 5 as a plot of the Ce³⁺ reduction current at $E_p^c = -1.34$ V (left-hand axis) versus the mole ratio of chloride to Ce³⁺, $m\text{Cl}^-/m\text{Ce}^{3+}$.

Interestingly, after the first small addition of chloride, the Ce³⁺ reduction current increases by about 15%. Close inspection of voltammograms labeled a and b in Figure 4 shows that whereas the reduction current increases, the current

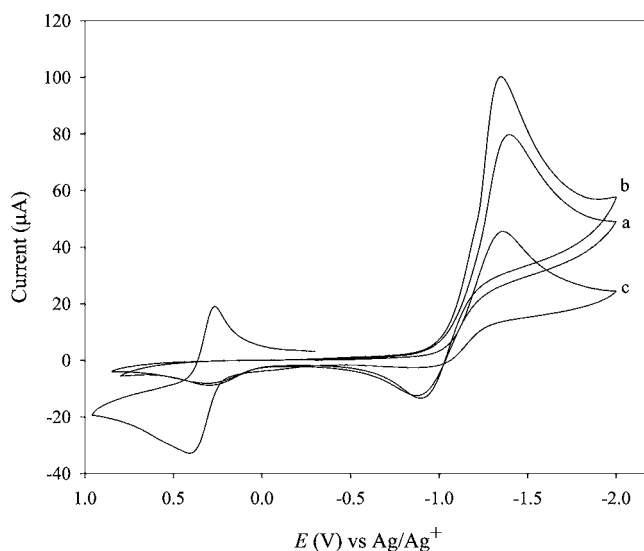


Figure 4. Cyclic staircase voltammograms recorded at a Pt electrode in BuMePyroTf₂N containing: (a) 0.095 M Ce³⁺, (b) 0.095 M Ce³⁺ + 0.110 M Cl⁻ ($m\text{Cl}^-/m\text{Ce}^{3+} = 1.1$), and (c) 0.095 M Ce³⁺ + 0.418 M Cl⁻ ($m\text{Cl}^-/m\text{Ce}^{3+} = 4.4$). The scan rates were 50 mV s⁻¹.

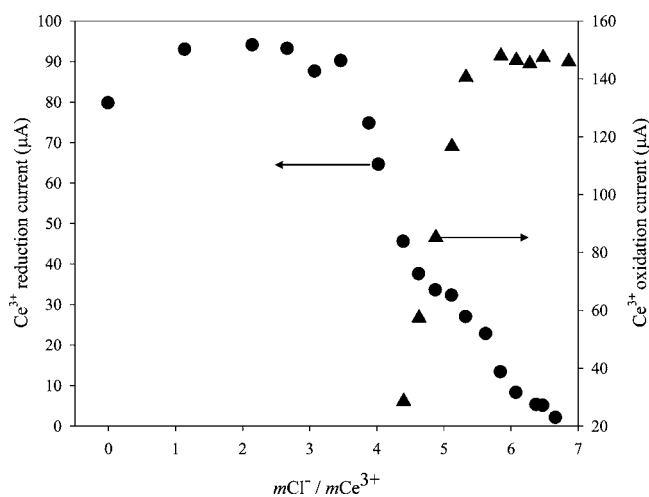


Figure 5. Plots of the Ce^{3+} voltammetric reduction current (left axis) and the Ce^{3+} oxidation current (right axis) versus $m\text{Cl}^-/m\text{Ce}^{3+}$ for the addition of Cl^- to a 0.095 M solution of Ce^{3+} in BuMePyroTf₂N. The scan rates were 50 mV s^{-1} .

for the oxidation of Ce^{2+} in the electrode diffusion layer does not change, that is, i_p^a/i_p^c actually becomes smaller as Cl^- is added to the solution. Clearly, the addition of small amounts of Cl^- increases the rate of the Ce^{2+} disproportionation reaction.³⁴ Further additions of chloride have little effect on the peak potential and current for the Ce^{3+} reduction wave until $m\text{Cl}^-/m\text{Ce}^{3+} \approx 3$. When $m\text{Cl}^-/m\text{Ce}^{3+} \geq 3$, the solution becomes permeated with a dispersed, finely divided white solid, and the Ce^{3+} reduction current begins to diminish.

Small amounts of the precipitate were recovered by centrifuging the ionic liquid. These samples were washed repeatedly with CH_2Cl_2 to remove as much of the ionic liquid as possible and dried under vacuum. Samples of this material were first evaluated with elemental chemical analysis. Although the results varied somewhat between samples, a typical result gave an empirical formula of $\text{C}_{1.16}\text{CeCl}_{2.44}\text{F}_{0.08}\text{H}_{1.01}\text{N}_{0.13}\text{O}_{1.53}\text{S}_{0.02}$. XRD analysis indicated that the precipitate was amorphous; therefore, it was examined with XPS. High-resolution photoemission spectra of the precipitate are shown in Figure 6 for the binding energy (BE) regions typically associated with Ce 3d, Cl 2p, and O 1s. The Ce 3d spectrum (Figure 6a) consists of two distinct bands at 886.0 and 904.6 eV corresponding to the $3d_{5/2}$ – $3d_{3/2}$ spin orbit doublet, as well as shoulders at 882.4 and 901.0 eV, respectively, which are typically attributed to charge transfer (CT) emission. The BE region for Cl 2p in Figure 6b shows two incompletely resolved bands at 198.3 and 200.0 eV corresponding to the $\text{Cl } 2p_{3/2}$ – $\text{Cl } 2p_{1/2}$ spin orbit doublet. These core level spectra are consistent with Ce^{3+} and Cl in CeCl_3 .^{35,36} We also examined the BE region associated with O 1s, and the results are shown in Figure 6c. In this case, the spectrum consists of a prominent band at 532 eV and a small shoulder at 529.7 eV. The first band was assigned to the O 1s emission from H_2O ^{37,38} and the shoulder was attributed to oxygen bonded to cerium in a cerium oxide compound, Ce_xO_y .³⁹

Taken together, the evidence presented above suggests that the precipitate obtained by adding chloride to the IL consists primarily of CeCl_3 with small amounts of entrapped residual IL, H_2O , and Ce_xO_y . The latter two species most likely originated from post processing of the precipitate because there is no

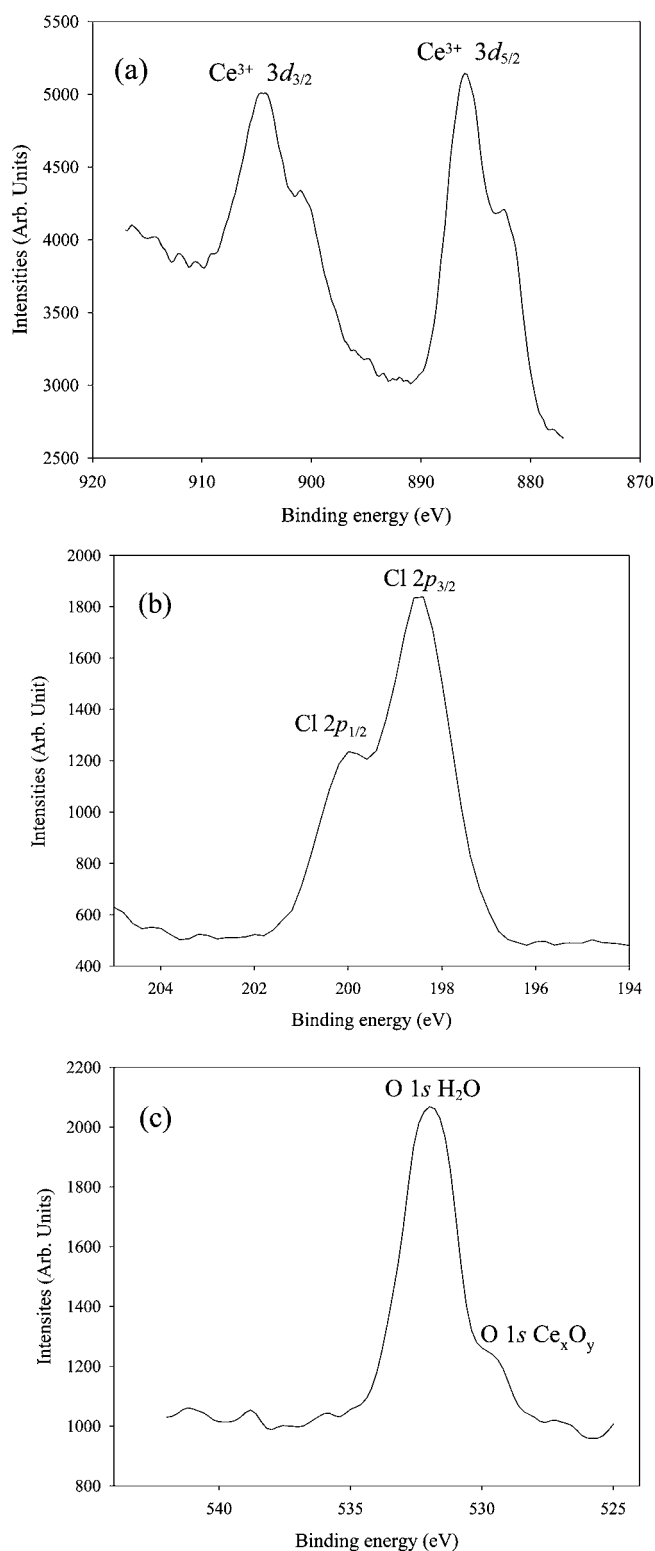


Figure 6. High resolution core-level photoemission spectra for the cerium precipitate: (a) Ce 3d, (b) Cl 2p, and (c) O 1s.

ready source of H_2O or oxygen in the very dry IL or glovebox atmosphere.

When $m\text{Cl}^-/m\text{Ce}^{3+}$ reaches 4.2, approximately 50% of the original Ce^{3+} has precipitated. The fact that not all of the Ce^{3+} has precipitated as CeCl_3 when $m\text{Cl}^-/m\text{Ce}^{3+} = 3$, suggests that the solubility product constant is fairly large. At this point in the titration, a voltammogram of the solution shows a new

oxidation wave and associated reduction wave at $E_p^a = 0.39$ V and $E_p^c = 0.27$ V, respectively (Figure 4c). These new voltammetric waves are assigned to the $Ce^{3+/4+}$ redox reaction. Thus, by virtue of the increased thermodynamic stability afforded to Ce^{3+} by complexation with chloride, the potential of the $Ce^{3+/4+}$ reaction has shifted cathodically and can now be observed within the potential window of the IL. The variation of the Ce^{3+} oxidation peak current as a function of mCl^-/mCe^{3+} is also shown in Figure 5, but on the right-hand axis. Figure 7 shows the evolution of the overall voltammetric

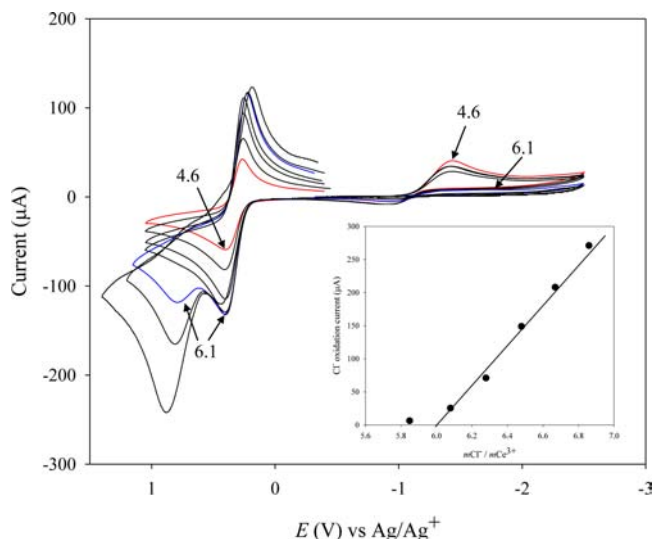


Figure 7. Cyclic staircase voltammograms recorded at a Pt electrode in BuMePyroTf₂N containing Ce³⁺ and chloride as a function of mCl^-/mCe^{3+} . The Ce³⁺ concentration was 0.095 M. Inset: plot of the chloride peak oxidation current versus mCl^-/mCe^{3+} . The scan rates were 50 mV s⁻¹.

signature of the Ce³⁺ solution with the addition of Cl⁻ as mCl^-/mCe^{3+} is varied from 4.6 to 6.5. The Ce³⁺ oxidation current continues to increase after each addition of Cl⁻ until $mCl^-/mCe^{3+} \sim 6$. When this ratio is attained, the Ce^{3+/2+} electrode reaction can no longer be observed within the potential window of the IL, the solution becomes completely clear, and no precipitate is visible. Subsequent additions of Cl⁻ for $mCl^-/mCe^{3+} > 6$ do not have any appreciable effect on the current for the Ce³⁺ oxidation wave, that is, the current reaches a constant value. However, it is now possible to observe a new oxidation wave at $E_p^a \approx 0.90$ V. The peak oxidation current for this wave increases as more chloride is added to the solution (Figure 7). This wave is attributed to the two-electron, quasireversible oxidation of chloride that is not coordinately bound to Ce³⁺, according to the reaction^{40,41}



The inset of Figure 7 shows that no free chloride is present in the solution until $mCl^-/mCe^{3+} > 6.0$.

Amperometric Titration: Addition of Ce³⁺ to Solutions of Cl⁻. To further explore the coordination of Ce³⁺ in solutions containing excess chloride, we carried out experiments in which Ce³⁺ was added coulometrically to BuMePyroTf₂N containing a fixed amount of BuMePyroCl. However, we first verified that the chloride oxidation current in these solutions varied linearly with the Cl⁻ concentration over the concentration range encountered during these experiments. (The electrochemistry

of Cl⁻ has been studied by Compton and co-workers^{41,42} in ionic liquids similar to that employed in this investigation and will not be discussed here.) Figure 8 shows voltammograms

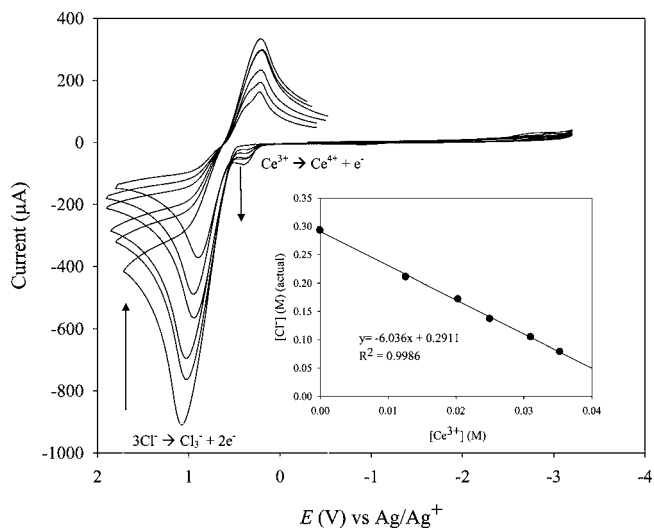


Figure 8. Cyclic staircase voltammograms recorded at a Pt electrode in a 0.30 M solution of chloride in BuMePyroTf₂N as a function of the Ce³⁺ concentration. Inset: Plot of the Cl⁻ concentration versus the Ce³⁺ concentration. The scan rates were 50 mVs⁻¹.

recorded after the coulometric addition of various amounts of Ce³⁺ to BuMePyroTf₂N initially containing a large excess of BuMePyroCl. In this figure, oxidation and reduction waves for chloride are apparent as well as small waves for the Ce^{3+/4+} reaction. As the concentration of Ce³⁺ in this solution increases, the oxidation wave for Cl⁻ decreases whereas that for Ce³⁺ increases. A plot of the chloride oxidation current versus the Ce³⁺ concentration constructed from this voltammetric data is given in the inset of this figure. The slope of this plot is 6.0, indicating that each Ce³⁺ must be complexed by six chlorides.

To verify the titration results, we also examined these solutions with electronic absorption spectroscopy. An absorption spectrum of Ce³⁺ in BuMePyroTf₂N with an excess of added chloride ($mCl^-/mCe^{3+} = 9$) is shown in Figure 9. This spectrum exhibits a single symmetrical band located at 332 nm (1640 l mol⁻¹ cm⁻¹) and is in close agreement with that reported for the octahedral chloride complex, [CeCl₆]³⁻, in CH₃CN saturated with Et₄NCl. In CH₃CN/Et₄NCl, the spectrum consists of a single band at 330 nm (1600 l mol⁻¹ cm⁻¹), which is attributed to a transition from the ground state ²F_{5/2} of [Xe]4f to the [Xe]5dγ₅ excited configuration.¹⁹ In view of the high concentration of Cl⁻ in these solutions and the observation of a spectroscopic signature consistent only with [CeCl₆]³⁻, it appears likely that this octahedral species is the limiting complex in this ionic liquid under the present conditions.

Electrochemistry of the [CeCl₆]^{3-/2-} Reaction in BuMePyroTf₂N. Cyclic staircase voltammetric data were collected for the [CeCl₆]^{3-/2-} reaction in a solution of [CeCl₆]³⁻ (Figure 10). This solution was prepared by the coulometric addition of Ce³⁺ to the neat ionic liquid and careful adjustment of mCl^-/mCe^{3+} to ~ 6 . The resulting solution contained no precipitate, no voltammetric waves could be detected for the reduction of Ce³⁺ or the oxidation of Cl⁻, and the absorption spectrum was identical to that in Figure 9.

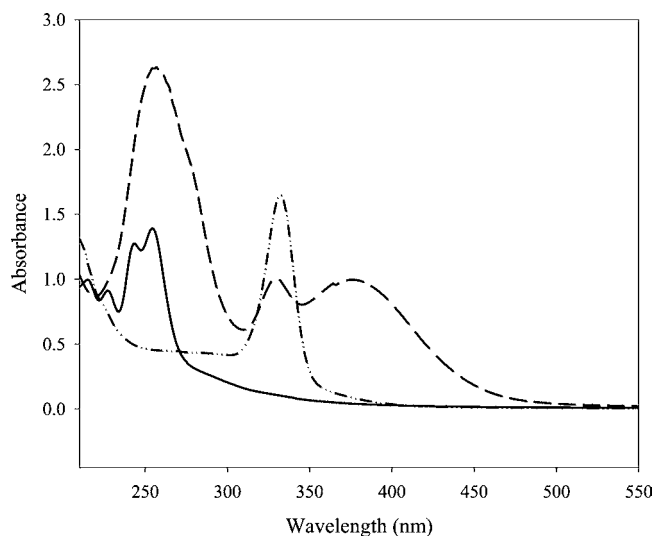


Figure 9. Electronic absorption spectra of Ce^{3+} recorded in BuMePyroTf₂N: (—) $[\text{Ce}(\text{Tf}_2\text{N})_x]^{(x-3)-}$, (---) $[\text{CeCl}_6]^{3-}$, and (-.-) solution of $[\text{CeCl}_6]^{2-}$ oxidized at 0.95 V.

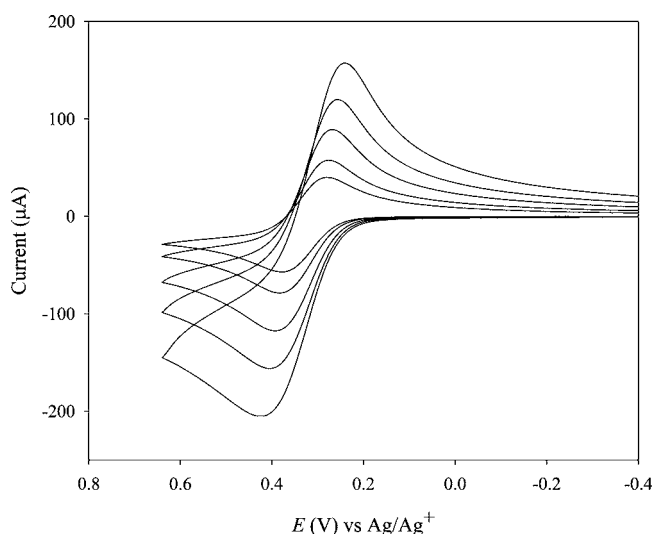


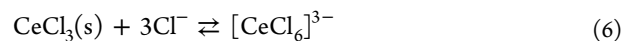
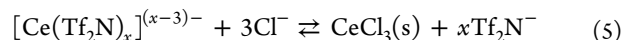
Figure 10. Cyclic staircase voltammograms recorded at a Pt electrode in BuMePyroTf₂N containing 0.095 M Ce^{3+} and chloride with $m_{\text{Cl}^-}/m_{\text{Ce}^{3+}} \approx 6$ as a function of scan rate: 0.010, 0.020, 0.050, 0.100, and 0.200 mV s^{-1} .

Voltammetric data resulting from these experiments are collected in Table 3. The peak current ratio, i_p^c/i_p^a , calculated by using Nicholson's empirical procedure,⁴³ was close to one for all of the scan rates tested, indicating that the $[\text{CeCl}_6]^{2-}$ produced by the oxidation of $[\text{CeCl}_6]^{3-}$ was chemically stable on the time scale of voltammetry. The data in Table 3 place the

voltammetric half-wave potential of the $[\text{CeCl}_6]^{3-/2-}$ reaction at 0.308 ± 0.008 V versus Ag^+/Ag or at about 0.25 V versus Fc/Fc^+ . The peak potential separation, ΔE_p , for this redox couple is greater than 100 mV over the range of scan rates examined, which is larger than the theoretical separation of 64 mV expected for a Nernstian reaction at 323 K. However, we hesitate to label this as a quasireversible reaction. This is because uncompensated solution resistance is problematic in modestly conducting ionic liquids such as BuMePyroTf₂N, even when standard electronic resistance compensation techniques are employed, leading to artificially large values of ΔE_p .⁴⁴ Thus, before this assignment can be made, this redox process must first be examined with a technique such as electrochemical impedance spectroscopy (EIS) that permits the discrimination of the solution and charge transfer resistances. An EIS investigation of the heterogeneous kinetics of the $[\text{CeCl}_6]^{3-/2-}$ reaction is outside the scope of this study and will be reported separately.

We attempted to prepare a solution of $[\text{CeCl}_6]^{2-}$ by coulometric oxidation of $[\text{CeCl}_6]^{3-}$ at an applied potential of 0.95 V at a large surface area Pt electrode. During the course of this experiment, the oxidation current decreased to a relatively small value, but did not reach the near zero value expected at the completion of an exhaustive electrolysis experiment. However, a spectrum of the solution resulting from these experiments (Figure 9) shows bands at 257 and 376 nm, which are in good correspondence with those at 255 and 376 nm reported for $[\text{CeCl}_6]^{2-}$ in CH_3CN saturated with Et_4NCl ,¹⁹ as well as a small band at 332 nm attributed to residual $[\text{CeCl}_6]^{3-}$. Thus, it is possible to prepare solutions that contain a preponderance of $[\text{CeCl}_6]^{2-}$ in neat BuMePyroTf₂N by controlled potential electrolysis, but this tetravalent cerium complex slowly reacts with the ionic liquid and does not exhibit long-term stability.

Taken together, the results presented above suggest the following sequence of reactions as chloride is added to a solution of Ce^{3+} in BuMePyroTf₂N



where the weakly solvated $[\text{Ce}(\text{Tf}_2\text{N})_x]^{(x-3)-}$ is first converted to the insoluble $\text{CeCl}_3(\text{s})$ and subsequently to the octahedrally coordinated $[\text{CeCl}_6]^{3-}$ complex. It is possible to obtain a rough estimate the solubility product, K_{sp} , of $\text{CeCl}_3(\text{s})$ in the IL from the data in Figure 5 at the point where the first obvious decrease in the $[\text{Ce}(\text{Tf}_2\text{N})_x]^{(x-3)-}$ reduction current is observed, that is, the point at which the IL becomes saturated with $\text{CeCl}_3(\text{s})$. This decrease is observed at $m_{\text{Cl}^-}/m_{\text{Ce}^{3+}} \approx 3.2$; here the concentrations of Ce^{3+} and Cl^- are 0.095 and 0.304 M, respectively, giving $K_{\text{sp}} \approx 2.7 \times 10^{-3}$.

Table 3. Cyclic Staircase Voltammetric Data for the $[\text{CeCl}_6]^{3-/2-}$ Reaction in BuMePyroTf₂N at 323 K

ν (V s^{-1})	E_p^a (V)	E_p^c (V)	ΔE_p	$E_{1/2}$ (V) ^a	i_p^c/i_p^a	$10^4 i_p/\nu^{1/2}$ ($\text{As}^{1/2} \text{V}^{-1/2}$)
0.01	0.380	0.280	0.100	0.300	1.0	5.70
0.02	0.384	0.276	0.108	0.304	1.1	7.86
0.05	0.392	0.268	0.124	0.308	1.1	11.8
0.10	0.408	0.256	0.152	0.312	1.2	15.6
0.20	0.424	0.240	0.184	0.316	1.2	20.4

^aEstimated from $E_{1/2} = (E_p^a + E_p^c)/2$.

The ability to effect the precipitation of at least some of the $\text{CeCl}_3(\text{s})$ by careful manipulation of $m\text{Cl}^-/m\text{Ce}^{3+}$ has positive implications for the processing of spent nuclear fuel with ILs. If it proves possible to apply these results to other trivalent lanthanides as well as tetravalent actinides, then chloride precipitation might serve as a simple route to recycling the expensive IL. Furthermore, the rare-earth chloride compounds produced by precipitation could be separated on the basis of their high temperature volatilities. Preliminary experiments involving the addition of Cl^- to solutions of Nd^{3+} and Pr^{3+} in BuMePyroTf₂N produced results very similar to those reported herein for Ce^{3+} . It is also noteworthy that experiments in which chloride was added to solutions of Np^{4+} and Pu^{4+} in BuMeImTf₂N also resulted in chloride-containing precipitates, but these amorphous solids were not identified.⁴⁵

In summary, we have examined the electrochemistry and coordination chemistry of Ce^{3+} in the BuMePyroTf₂N ionic liquid. Spectroscopic results indicated that Ce^{3+} was weakly solvated by Tf₂N⁻ ions as $[\text{Ce}(\text{Tf}_2\text{N})_x]^{(x-3)-}$, $x \geq 3$ in the neat solvent. This species can be reduced to a related Ce^{2+} species, but the latter exhibits only transient stability and quickly disproportionates to Ce^{3+} and Ce^0 ; the latter appears to react with the ionic liquid to form an electrode surface film. The addition of Cl^- to solutions of $[\text{Ce}(\text{Tf}_2\text{N})_x]^{(x-3)-}$ first causes the precipitation of $\text{CeCl}_3(\text{s})$. However, the $\text{CeCl}_3(\text{s})$ redissolves as the octahedral complex, $[\text{CeCl}_6]^{3-}$, when $m\text{Cl}^-/m\text{Ce}^{3+}$ is increased above 3. The $[\text{CeCl}_6]^{3-}$ can be coulometrically oxidized to $[\text{CeCl}_6]^{2-}$, which exhibits modest stability in the ionic liquid.

AUTHOR INFORMATION

Corresponding Author

*E-mail: chclh@chem1.olemiss.edu.

Notes

The authors declare no competing financial interest.

ACKNOWLEDGMENTS

This research was funded by the Division of Chemical Sciences, Geosciences, and Biosciences, Office of Basic Energy Science of the U.S. Department of Energy through Grant DE-AC02-98CH10886, Subcontract 154868, from Brookhaven National Laboratory

REFERENCES

- (1) Ohno, H. *Electrochemical Aspects of Ionic Liquids*; John Wiley & Sons: Hoboken, NJ, 2005.
- (2) Endres, F. *Electrodeposition from Ionic Liquids*; Wiley-VCH: Weinheim, Germany, 2008.
- (3) Tsuda, T.; Hussey, C. L. *Interface* **2007**, *16*, 42–49.
- (4) Tsuda, T.; Hussey, C. L. In *Modern Aspects of Electrochemistry*; White, R. E., Ed.; Springer Science: 2009; Vol. 45, pp 63–174.
- (5) MacFarlane, D. R.; Meakin, P.; Sun, J.; Amini, N.; Forsyth, M. J. *Phys. Chem. B* **1999**, *103*, 4164–4170.
- (6) Chen, P. Y.; Hussey, C. L. *Electrochim. Acta* **2004**, *49*, 5125–5138.
- (7) Pan, Y.; Boyd, L. E.; Kruplak, J. F.; Cleland, W. E.; Wilkes, J. S.; Hussey, C. L. *J. Electrochem. Soc.* **2011**, *158*, F1–F9.
- (8) Appleby, D.; Hussey, C. L.; Seddon, K. R.; Turp, J. E. *Nature* **1986**, *323*, 614–616.
- (9) Ha, S. H.; Menchavez, R. N.; Koo, Y.-M. *Korean J. Chem. Eng.* **2010**, *27*, 1360–1365.
- (10) Sun, X.; Luo, H.; Dai, S. *Chem. Rev.* **2011**, *112*, 2100–2128.
- (11) Binnemans, K. *Chem. Rev.* **2007**, *107*, 2592–2614.

(12) Venkatesan, K. A.; Rao, C. J.; Nagarajan, K.; Rao, P. R. V. *Int. J. Electrochem* **2012**, *2012*, 12.

(13) Cocalia, V. A.; Gutowski, K. E.; Rogers, R. D. *Coord. Chem. Rev.* **2006**, *250*, 755–764.

(14) Shannon, R. D. *Acta Crystallogr.* **1976**, *A32*, 751–767.

(15) Poml, P.; Geisler, T.; Cobos-Sabate, J.; Wiss, T.; Raison, P. E.; Schmid-Beurmann, P.; Deschanel, X.; Jegou, C.; Heimink, J.; Putnis, A. *J. Nucl. Mater.* **2011**, *410*, 10–23.

(16) Mehdi, H.; Bodor, A.; Lantos, D.; Horvath, I. T.; De Vos, D. E.; Binnemans, K. *J. Org. Chem.* **2007**, *72*, 517–524.

(17) Lin, F. M.; Hussey, C. L. *J. Electrochem. Soc.* **1993**, *140*, 3093–3096.

(18) Mills, A.; Cook, A. *J. Chem. Soc., Faraday Trans. 1* **1988**, *84*, 1691–1701.

(19) Ryan, J. L.; Jorgensen, C. K. *J. Phys. Chem.* **1966**, *70*, 2845–2857.

(20) Rao, C. J.; Venkatesan, K. A.; Nagarajan, K.; Srinivasan, T. G.; Rao, P. R. V. *J. Nucl. Mater.* **2010**, *399*, 81–86.

(21) Chandra, M.; Vandarkuzhali, S.; Ghosh, S.; Gogoi, N.; Venkatesh, P.; Seenivasan, G.; Reddy, P. B.; Nagarajan, K. *Electrochim. Acta* **2011**, *58*, 150–156.

(22) Williams, D. B.; Stoll, M. E.; Scott, B. L.; Costa, D. A.; Oldham, W. J. *Chem. Commun.* **2005**, 1438–1440.

(23) Galliard, C.; Billard, I.; Chaumont, A.; Mekki, S.; Ouadi, A.; Denecke, M. A.; Moutiers, G.; Wipff, G. *Inorg. Chem.* **2005**, *44*, 8355–8367.

(24) Babai, A.; Mudring, A. V. *Chem. Mater.* **2005**, *17*, 6230–6238.

(25) Babai, A.; Mudring, A. V. *Dalton Trans.* **2006**, 1828–1830.

(26) Wilkes, J. S.; Levisky, J. A.; Wilson, R. A.; Hussey, C. L. *Inorganic Chemistry* **1982**, *21*, 1263–1264.

(27) Jorgensen, C. K.; Brinen, J. S. *Mol. Phys.* **1963**, *6*, 629–631.

(28) Billard, I.; Gaillard, C. *Radiochim. Acta* **2009**, *97*, 355–359.

(29) Bhatt, A. I.; May, I.; Volkovich, V. A.; Collison, D.; Helliwell, M.; Polovov, I. B.; Lewin, R. G. *Inorg. Chem.* **2005**, *44*, 4934–4940.

(30) Yamagata, M.; Katayama, Y.; Miura, T. *J. Electrochem. Soc.* **2006**, *153*, E5–E9.

(31) Rao, C. J.; Venkatesan, K. A.; Nagaishi, R.; Srinivasan, T. G.; Rao, P. R. V. *Electrochim. Acta* **2009**, *54*, 4718–4725.

(32) Brown, E.; Sandifer, J. R. In *Electrochemical Methods, Physical Methods of Chemistry Vol. II*; Rossiter, B. W., Hamilton, J. F., Eds.; John Wiley & Sons: New York, 1986; pp 322–324.

(33) Lewandowski, A.; Swiderska-Moock, A. *J. Power Sources* **2009**, *194*, 601–609.

(34) Ohmstead, M. L.; Nicholson, R. S. *Anal. Chem.* **1969**, *41*, 862–864.

(35) Park, K.-H.; Oh, S.-J. *Phys. Rev. B* **1993**, *48*, 14833–14842.

(36) Giuffrida, S.; Condorelli, G. C.; Costanzo, L. L.; Ventimiglia, G.; Favazza, M.; Petralia, S.; Fragala, I. L. *Inorg. Chim. Acta* **2006**, *359*, 4043–4052.

(37) Coenen, F. P.; Kastner, M.; Pirug, G.; Bonzel, H. P. *J. Phys. Chem.* **1994**, *98*, 7885–7890.

(38) Ciba, K.; Ohmori, R.; Tanigawa, H.; Yoneoka, T.; Tanaka, S. *Fusion Eng. Des.* **2000**, *49–50*, 791–797.

(39) Rack, P. D.; O'Brien, T. A.; Zerner, M. C.; Holloway, P. H. *J. Appl. Phys.* **1999**, *86*, 2377–2384.

(40) Villagran, C.; Banks, C. E.; Deetlefs, M.; Driver, G.; Pitner, W. R.; Compton, R. G.; Hardacre, C., In *Ionic Liquids IIIb: Fundamentals, Progress, Challenges and Opportunities: Transformations and Processes*; American Chemical Society: Washington, DC, 2005; Vol. 902, pp 244–258.

(41) Aldous, L.; Silvester, D. S.; Villagran, C.; Pitner, W. R.; Compton, R. G.; Lagunas, M. C.; Hardacre, C. *New J. Chem.* **2006**, *30*, 1576–1583.

(42) Villagran, C.; Banks, C. E.; Hardacre, C.; Compton, R. G. *Anal. Chem.* **2004**, *76*, 1998–2003.

(43) Nicholson, R. S. *Anal. Chem.* **1966**, *38*, 1406.

(44) Pan, Y.; Hussey, C. L. *J. Electrochem. Soc.* **2012**, *159*, F125–F133.

(45) Nikitenko, S. I.; Moisy, P. *Inorg. Chem.* **2006**, *45*, 1235–1242.